Los Alamos
Los Alamos National Laboratory
Los Alamos, New Mexico 87545

memorandum

TO: Distribution

DATE: September 27, 1982

FROM: D. Brown, H. Keppler, M. Kuriyagawa
H. Murphy, and Fritz Walter

MAIL STOP/TELEPHONE: J981/7-4318

SYMBOL: ESS-4-82-421

SUBJECT: FRACTURING EXPERIMENT 2016

Summary

Experiment 2016 was conducted on June 20 and 21, 1982. This experiment represented our third attempt at a fracture connection between the bottom of hole EE-2, and the openhole section of EE-3. The initial fractures formed in the 450-foot-long openhole interval below the cemented-in liner in EE-2 were first extended during the 130,000 gallon injection of Experiment 2011. Following a 5-day intervening vent period, further pumping during Experiment 2012 -- 800,000 gallons of total injected flow -- extended the seismic fracture zone to the region of EE-3, but without any indication of fracture breakthrough. The primary objective of Expt. 2016 was to hydraulically connect holes EE-2 and EE-3, utilizing a greater amount of injected fluid -- 1.3 million gallons were pumped into EE-2 -- and somewhat higher injection rates up to 35 BPM (as compared to 30 BPM during Expt. 2012). Despite this large volume of injected water, we failed to achieve hydraulic communication with EE-3.

Extensive downhole measurements of the locations of microseismic events generated during the hydraulic fracturing process were made during this experiment, utilizing a three-axis oriented geophone package positioned at a depth of about 9700 feet in EE-1. These microseismic data may explain why we failed to connect the two wellbores. The data suggest three distinct -- but parallel -- fracture zones, inclined at about 45° from the vertical, and extending upwards and to the east away from EE-3 (these fracture zones strike roughly north-south, and dip about 45° to the west). The injection-pressure/flow-rate data from Expts. 2011 and 2016 support the existence of multiple fractures intersecting the openhole section of EE-2. Since, hole EE-3 was drilled somewhat short of being directly above the bottom of hole EE-2, these fracture zones may have all missed the bottom of EE-3.

The mean fracture closure stress, obtained from analyses of the wellhead shut-in pressure decay data associated with four separate pump shutdown events, is 376 bars (5450 psi). This corresponds to a total closure stress of 806 bars (11,680 psi) at the middle of the openhole section below the liner, at a true vertical depth of 4.31 km (14,100 feet). Based on stress measurements in the Phase I reservoir, this closure stress level would indicate that these fracture zones should be inclined 40° from the vertical -- in good agreement with the seismic results given above. In addition, with this inclination to the principal stress directions, these fracture zones should have generated significant shear events under pressurization.

A chronology of significant events during Expt. 2016 is given in Table I. Figure 1 summarizes the injection pressure (measured at the surface) and injection flow rate as functions of time.

Microseismic Fracture Location Results (H. Keppler and C. Pearson)

The majority of the microseismic results from Expt. 2016 were obtained from the oriented geophone package located in hole EE-1 at a depth of 2950 m (9670 feet). The accelerometer package was not on station in hole EE-3 until 00:24 on Monday morning (6-21-82), just 47 minutes before flow was shutdown at 01:11.

Significant seismic activity -- but at an initially low event rate -- began at about 10:00 on June 20, after having injected a total of about 320,000 gallons into EE-2. These early microearthquakes occurred roughly 450 m east of the termini of holes EE-2 and EE-3, and at a vertical depth of about 3700 m (12,000 feet) as shown in Fig. 2. Subsequently, seismic activity increased and spread on an oblate region dipping between 30° and 60° from the vertical (towards the west), and striking roughly perpendicular to the wellbore direction. Figure 3 shows a typical time interval displaying this feature, which could be observed until around 15:00. Significantly, there were almost no seismic signals originating from the vicinity of the bottom of EE-3 during this time interval. In comparison, recall that seismicity in Expt. 2012 started below the injection interval of EE-2 as shown in the elevation view of Fig. 4, and later concentrated on a second inclined (40° from the vertical) feature surrounding the bottom 200 m of EE-3.

After 15:00 the locations of the microearthquake origins started spreading out, with a slight trend towards the southwest with deeper foci

TABLE I

Experiment 2016
Sunday, June 20, 1982

Time	
01:14	Pumping Started, 5 BPM
04:40	Pressure stabilized at 5890 psi; flow = 200.3 gpm
04:48	Flow Increased to 10 BPM
04:50	So far, only 2 bbls vented from backside
06:30	Flow Increased to 15 BPM
07:15	Flow Increased to 20 BPM
07:37	Going up to 30 BPM
09:04	1 BPM backside vent rate
10:20	300-mesh silica flour going in
11:48	Pumps Down; lost blender suction (ISIP = 5530 psi)
13:06	Flow coming up again
13:07	21 BPM
13:23	30 BPM
14:00	31 BPM, 540,000 gallons injected
15:42	1.0 BPM backside vent rate
16:15	Bad leak past pipe rams: Shutting down (ISIP = 5470 psi)
16:34	Closed hydrill; Pumping again
17:01	Shut down to replace pipe rams for safety considerations (ISIP = 5400 psi)
18:57	Flow coming up again
19:08	16 BPM; 770,000 gallons injected
19:21	Flow up to 35 BPM
20:00	34 BPM; 840,000 gallons injected
21:00	34 BPM; 924,000 gallons injected
23:00	34 BPM; 1,100,000 gallons injected
00:24	Accelerometer on station (12,500 feet)
01:11	Dowell shut down (ISIP = 5420 psi)

Figure 1

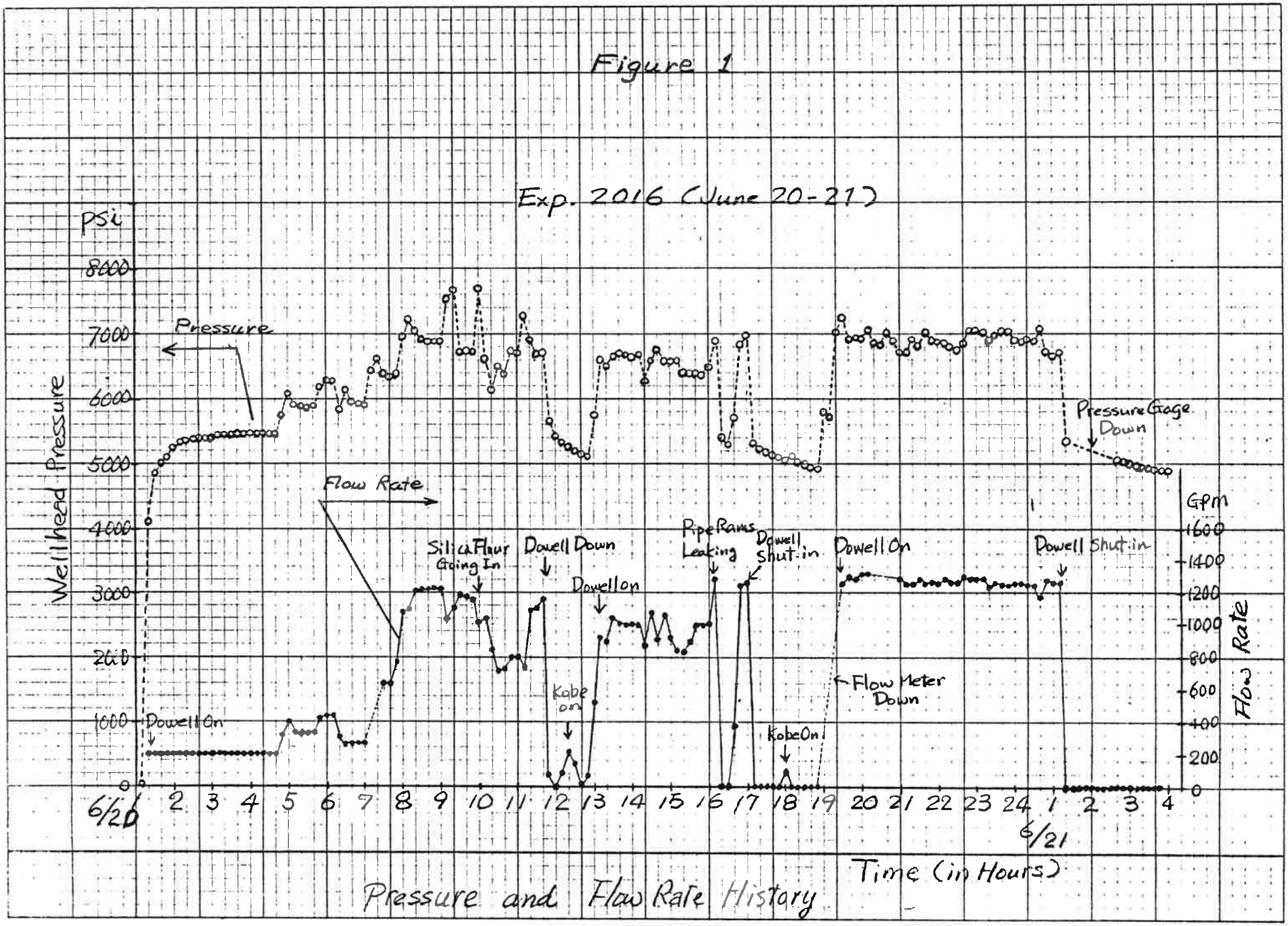

Pressure and Flow Rate History

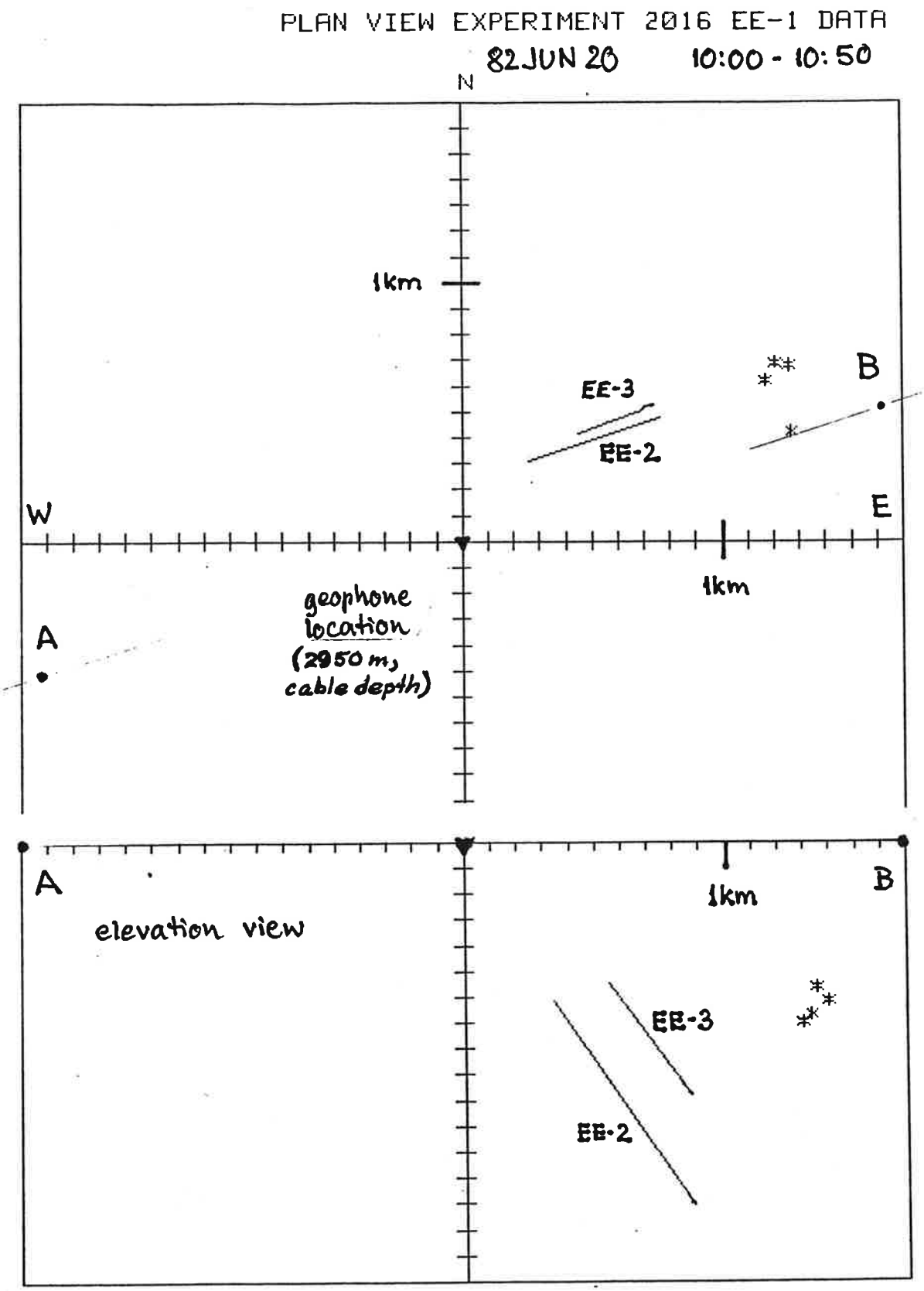

Figure 2. Hypocenters (asterisks) of the first microearthquake signals detected with the geophone tool in EE-1. Plan view (upper) figure and projection to the vertical AB plane (lower) are shown.

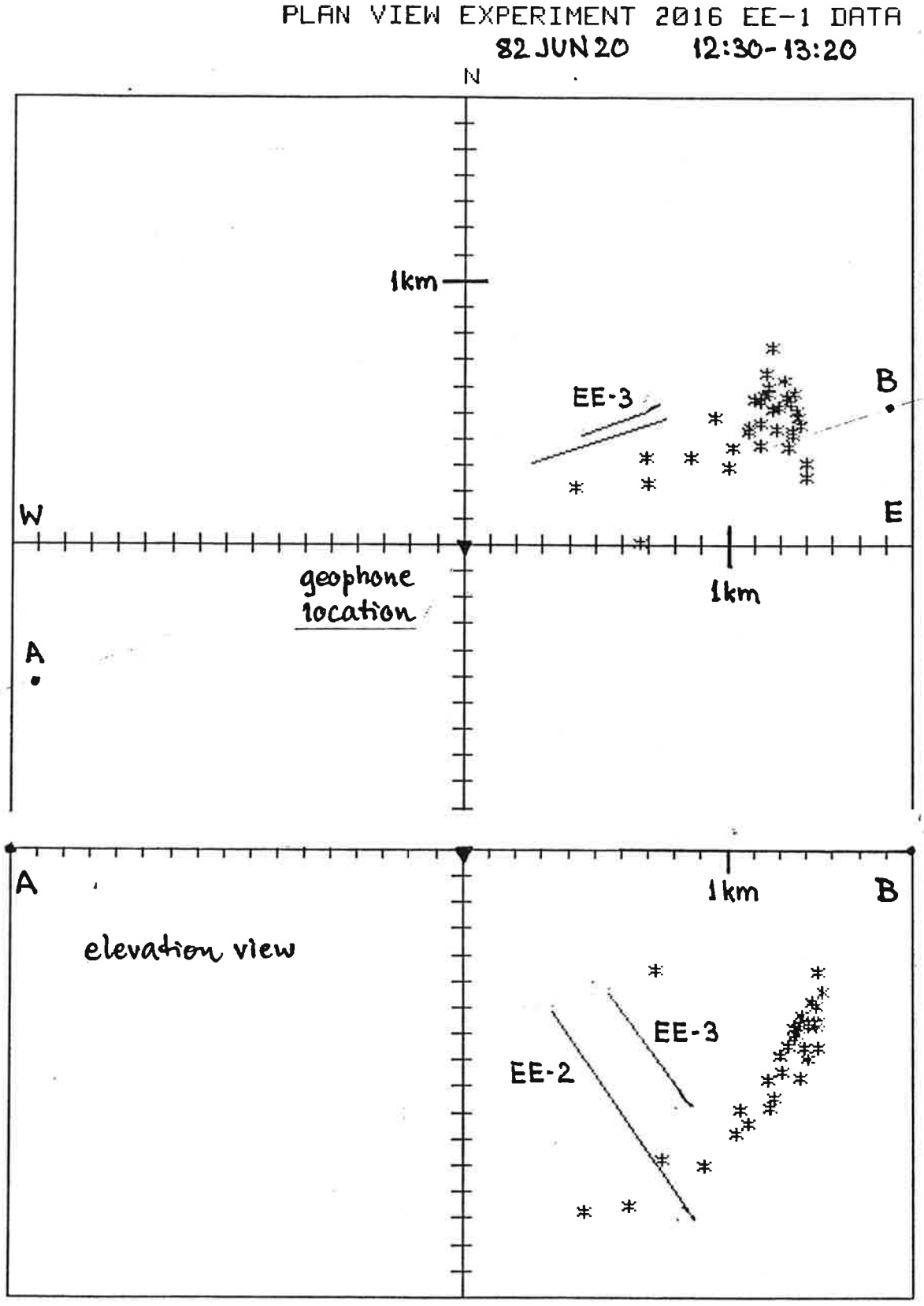

Figure 3. Hypocenters of microearthquakes for the time between 10:00 and 15:00, when seismicity occurred in a narrow, inclined region.

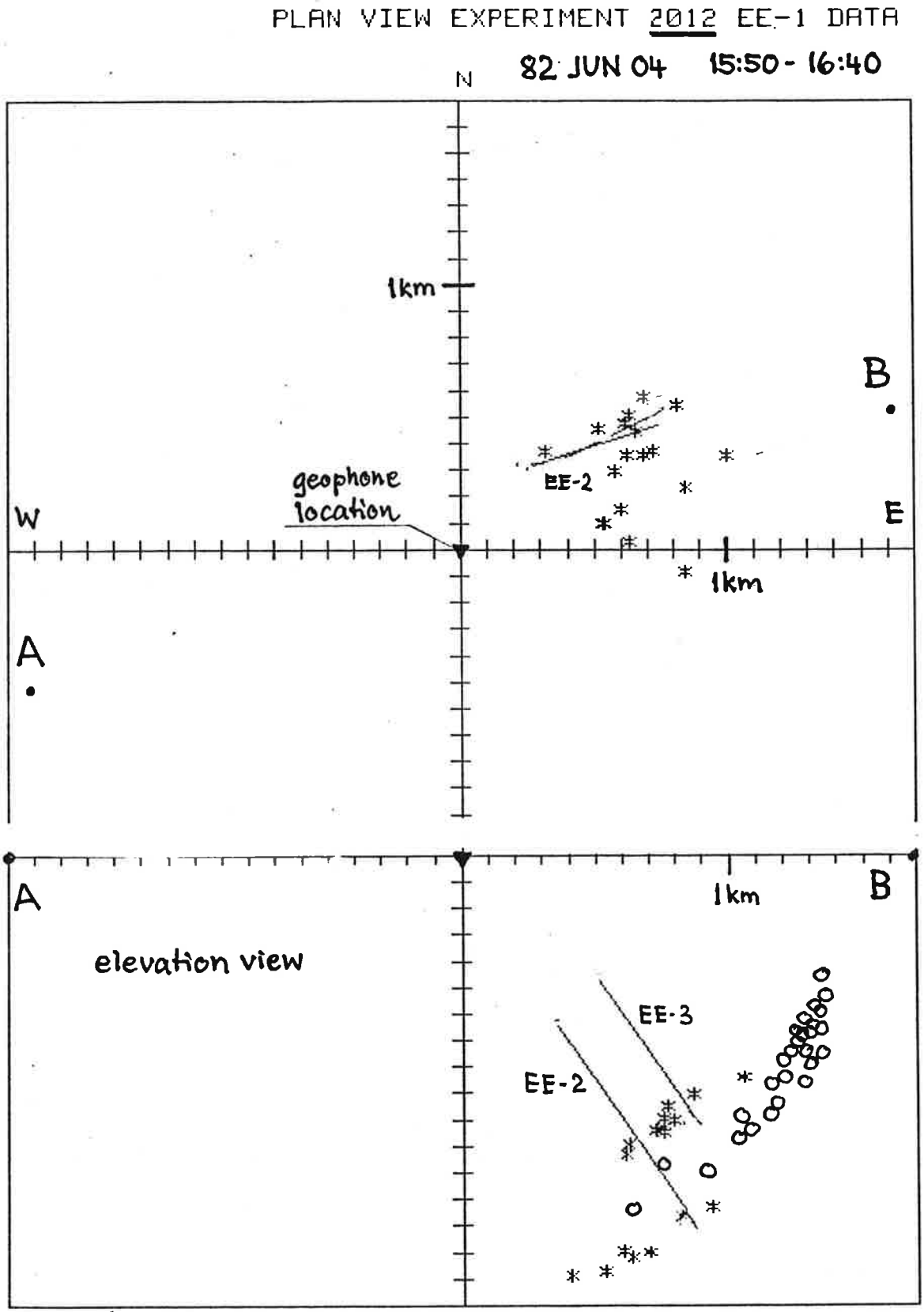

Figure 4. Comparison of two 50 minute intervals from Experiment 2012 (asterisks) and Experiment 2016 (circles) in projection to vertical AB plane.

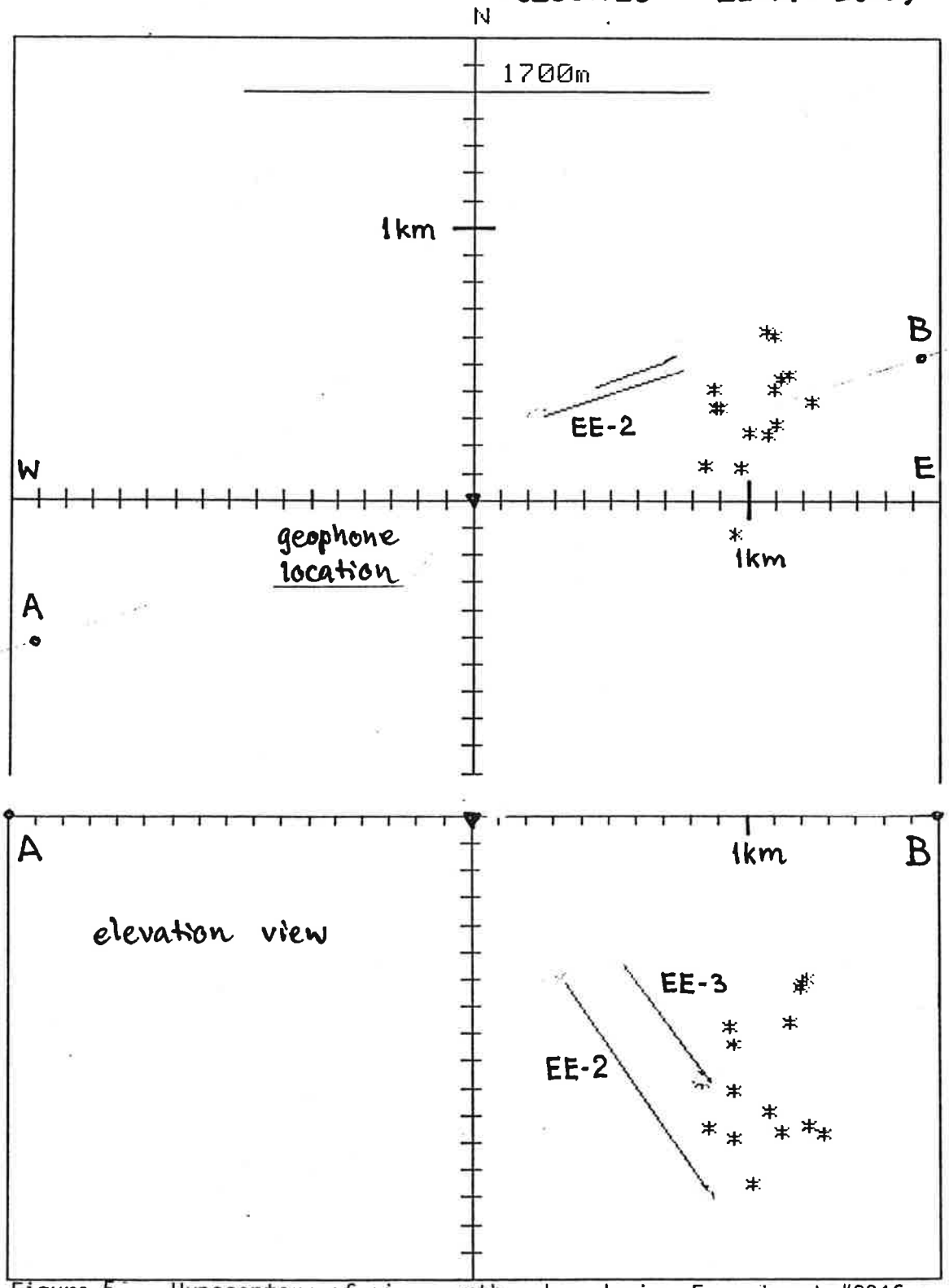

Figure 5. Hypocenters of microearthquakes during Experiment #2016. Last time interval processed at Fenton Hill during the experiment.

(see example in Fig. 5). We ceased active investigation at 01:00 (June 21) at which time events occurring as late as 23:00 (June 20) had been included in the on-the-spot analysis. At that time, there was no evidence of a dense clustering of hypocenters in areas that might indicate a feature that would connect the wellbores.

On June 21 at 00:39 the first signal was recorded with both the accelerometer and geophone tools. The accelerometer was locked in at a 12,500 ft (3810 m) cable depth [11,890 ft (3625 m) TVD] in EE-3. The S-P times predicted for this accelerometer position from previous locations with the geophone tool alone ranged from 0 to 110 ms. S-P times read from accelerograms ranged from 48.7 ms to 100.0 ms and thus confirmed the geophone microseismic event locations to the east and beyond the bottom of EE-3.

The precision of the locations from the EE-1 geophone signals are within ± 25 m in the radial direction, stemming from a reading inaccuracy for the S-P times of less than 3 ms. The repeatability of the hodogram analysis yields an error cone with a typical apex angle of 14°; this results in a lateral precision of ± 200 m. It must be emphasized that this precision is sufficient to resolve the above-mentioned features (compare Fig. 5).

We can't quantify a possible systematic error, due to our tool orientation inaccuracy stemming from both the misalignment (probably small) of the inclinometers and the uncertainty of the wellbore surveys. From the repeatability of the azimuths between different experiments, we feel that the error is within ± 10°.

Analysis of the Fracture Closure Stress (D. Brown and M. Kuriyagawa)

There were four significant flow shutins during Expt. 2016, as shown in Fig. 1 and listed in Table I. These four sets of shutin pressure decay data were used to infer the mean fracture closure stress near the bottom of EE-2: i.e., that downhole pressure level required to inject significant amounts of fluid into the set of inclined fractures intersecting the EE-2 wellbore below the cemented-in liner. Table II summarizes the analysis of these four sets of shutin data. The first column lists the instantaneous shutin pressure (ISIP)* as obtained from curve-fitting the analog pressure

* The surface injection pressure without pipe friction losses.

plots. The second column lists the shutin pressure obtained by a Muskat* curve fit to the digital data (unfortunately, in each case, the digital data were averaged over two-minute time intervals, so it was difficult to pick an accurate shutin time.) One representative Muskat fit is shown in Fig. 6, for the surface pressure decay data following the first wellbore shutin at 11:48.

Table II

Instantaneous Shutin Pressures From Experiment 2016
(in psi)

	Curve Fit to Analog Data	Muskat Fit to Digital Data
First Shutin, 11:48	5530	5420
Second Shutin,16:15	5470	----
Third Shutin, 17:01	5400	5510
Fourth Shutin,01:11	5420	5450
Average	5450	5460

From the above table, it is apparent that the mean instantaneous reservoir shutin pressure was 5450 psi during the majority of Experiment 2016, and was apparently not time dependent: i.e., the internal fracture pressure was not decreasing with time. With a mean slant depth for the openhole interval of 14,900 feet (true vertical depth of 14,100 feet) and a mean wellbore fluid density (cold) of 1.018 gm/cc, this corresponds to a total donwhole pressure of 11,680 psi (hydrostatic pressure = 6230 psi).

*Muskat, Morris, "Use of Data on the Build-up of Bottom-Hole Pressures," in SPE Reprint Series No. 9: Pressure Analysis Methods, Society of Petroleum Engineers of the AIME, 1967.

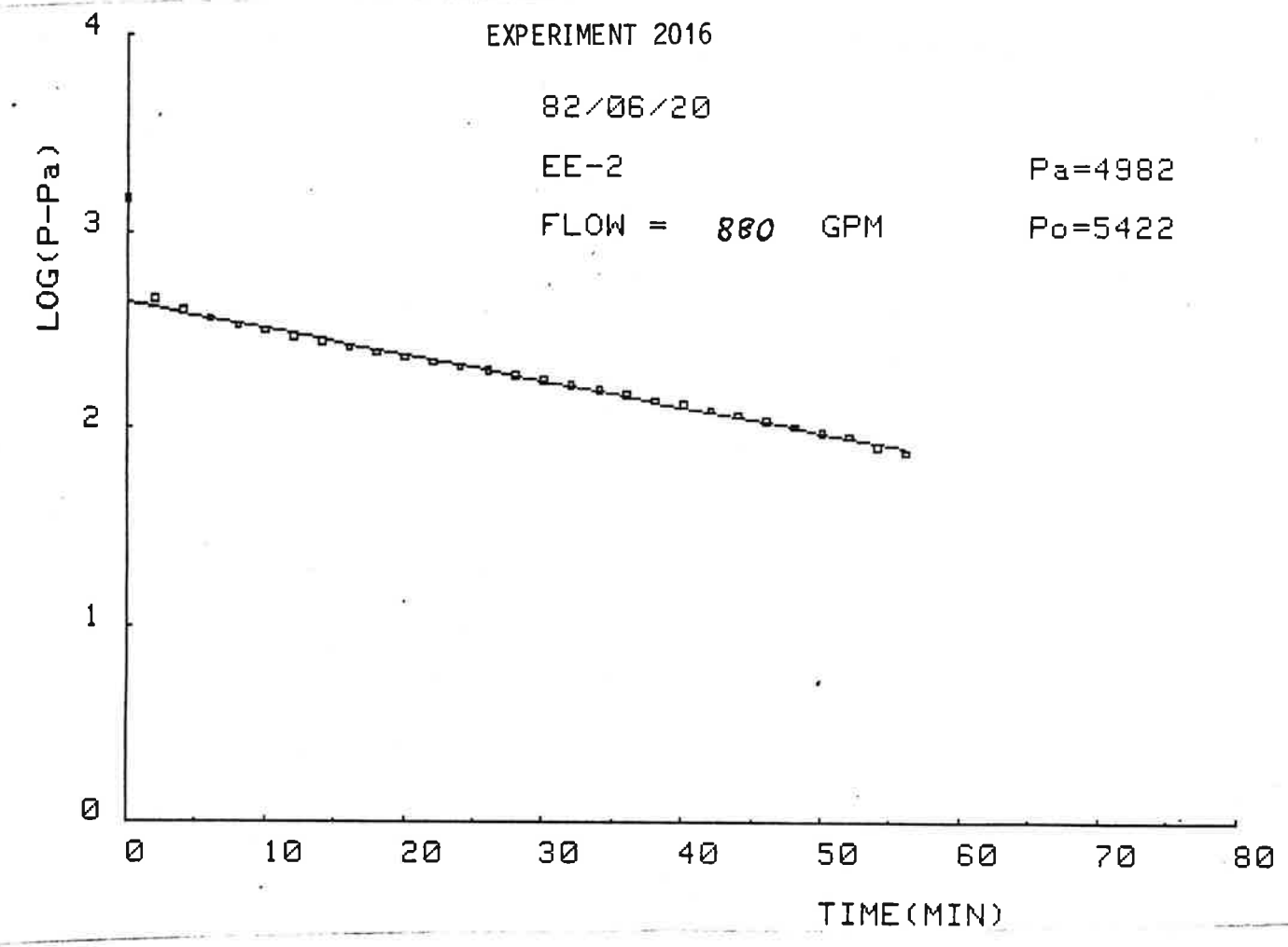

Figure 6. Muskat Technique for Analyzing Pressure Decay During 1st Shut-in.

Fracture Injection Pressure as a Function of flow Rate (D. Brown)

During injection flow testing of the upper part of the Phase I reservoir in 1976 (Expt. 117), a linear relationship was obtained between surface injection pressure and flow rate. This linear correlation, for the major EE-1 fracture inlet at a depth of 9050 feet, is replotted in Fig. 7 for reference.

During Expts. 2011 and 2016 in the Phase II system, similar linear relationships were obtained between injection pressure and flow rate, but with a unique feature: an apparent horizontal shift of the curve to higher flow rates at the same pressures for Expt. 2016, as compared to Expt. 2011. This displacement between the two curves can be interpreted as resulting from a significant increase in the flow cross-sectional area -- i.e., the number of fractures that had opened -- between these two experiments. The pertinent data, and supporting information, are given in Fig. 8.

From the data presented, it appears that only one fracture (or set of fractures) was opened during the 130,000 gallon injection of Expt. 2011. This conclusion is supported by the microseismic data obtained from Expt. 2011, which showed a narrow seismic zone extending both upwards and downwards from near the bottom of the EE-2 openhole interval below the cemented-in PBR/liner. In addition, the extended 5 BPM flow plateau at the beginning of Expt. 2012 correlates with the Expt. 2011 pressure/flow-rate curve, indicating that the one-fracture-zone condition persisted through the early phase of Expt. 2012.

Although obviously only qualitative, the data of Fig. 8 suggest that several additional fracture zones may have been opened during the much higher (than Expt. 2011) injection flow rate and downhole fracture inlet pressure conditions existing during the latter portions of Expt. 2012. That additional fractures had been opened prior to Expt. 2016 is also suggested by the 110 psi increase in the instantaneous shutin pressure (ISIP) between Expts. 2011 and 2016, as shown in Fig. 8. This pressure increase would indicate the presence of at least one additional fracture zone with a somewhat higher fracture closure stress: either a deeper one, or one with a slightly lower inclination.

Figure 7

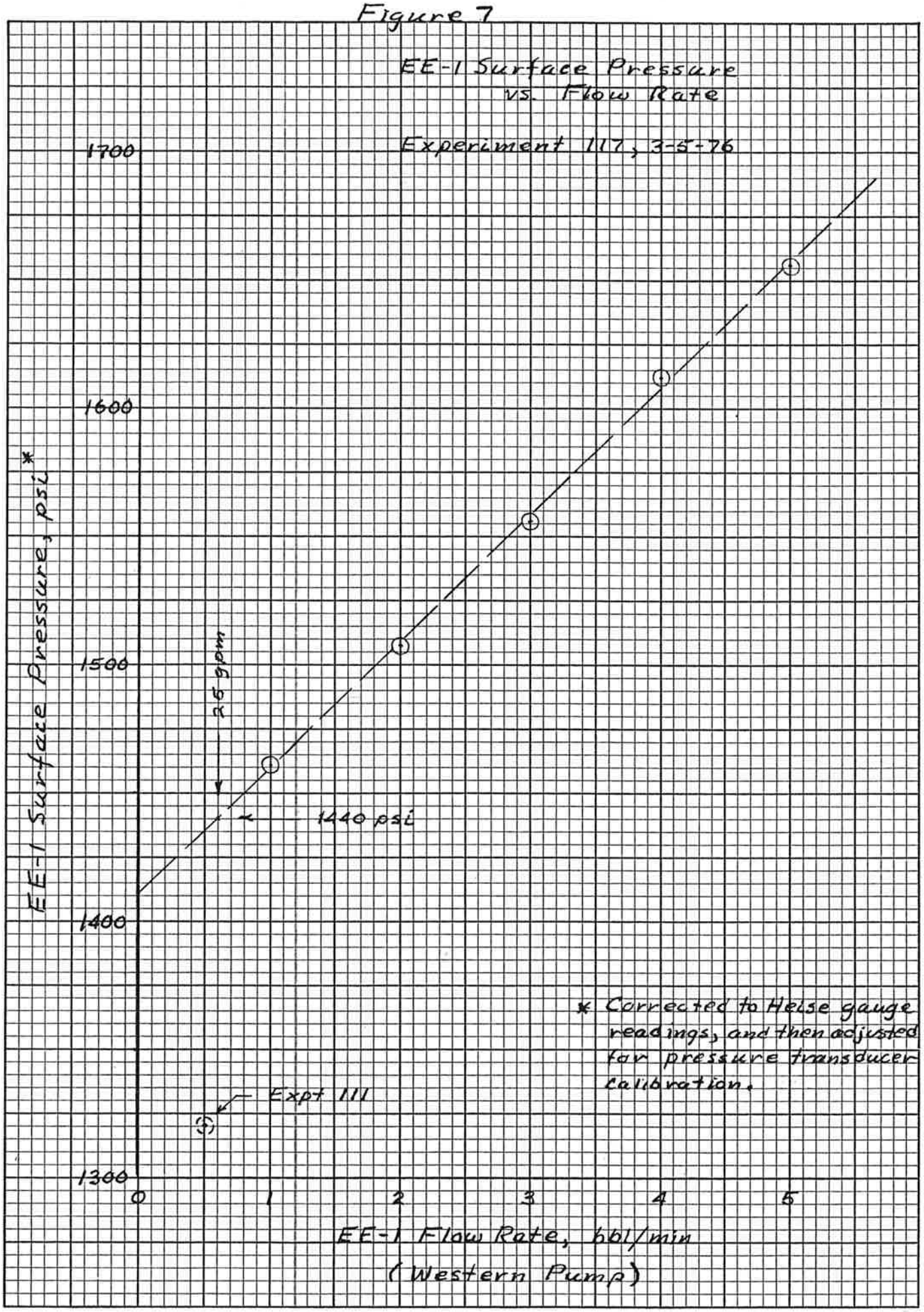

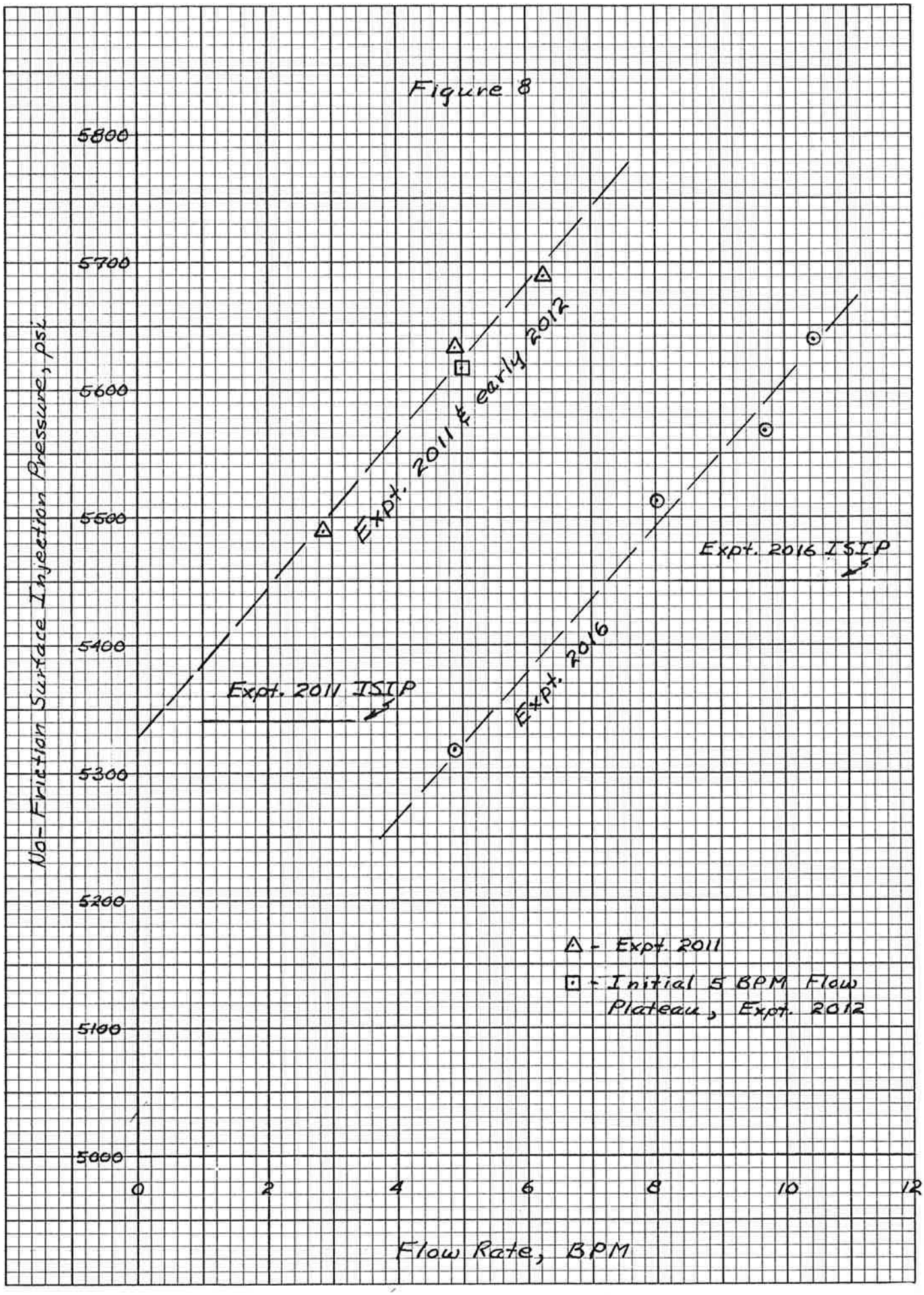

Presence of at Least One Manifolding Joint (D. Brown)

There is evidence for the existence of at least one "manifolding" joint near the bottom of EE-2, which interconnects the primary set of inclined fractures that were pressurized and extended during Expt. 2016. From the elevation view of the microseismic event locations shown in Fig. 4, the upper Expt. 2012 seismic trend (asterisks) crosses the EE-2 wellbore about 1200 feet (370 m) from the bottom of the hole, as measured along the wellbore. Therefore, this active microseismic zone intersects the EE-2 wellbore 260 feet above the top of the cemented-in liner, precluding its direct pressurization through the frac string. To have activated this upper seismic zone requires that the fracture flow entering the lower openhole interval must have moved upwards along an aseismic joint or joints, roughly parallel to the trace of EE-2, and truncated by the set of inclined fractures. A set of pre-existing (before the inclined fracture set was formed) S_2 joints would satisfy all the above conditions:

1. An S_2 joint implies a shear-free pressurization.
2. The strike of the S_2 joints in the phase I reservoir was roughly east-west.
3. The S_2 joint closure stress should be about 4100 psi, not too far below the inclined-fracture-set closure stress of 5450 psi, but very adequate to provide a low-impedance interconnection path.

Liner Bypass Flow Analysis (M. Kuriyagawa, F. Walter, and D. Brown)

During the duration of Expt. 2016, the annulus outside the frac string (backside) first had to be pressurized, then shut in, and finally vented to maintain the pressure between about 1600 and 2000 psi (to minimize the pressure difference across the PBR seals). This annulus pressure control was accomplished by using a "backside" pump truck (used to provide the initial pressurization) and a vent valve.

Fig. 9 shows the time-variation of the annulus surface pressure and flow rate. Following the initial pressurization, the annulus was intermittently pressurized for the next 3 hours to compensate for the cooling-induced density increase of the annulus fluid. For the next 1-1/2 hours, the annulus was mostly shut in. Finally, about 5 hours after the initiation of fracture injection flow, it was necessary to start continuously venting the annulus to maintain the pressure below 2000 psi. About 10 hours after the initiation of fracture injection flow, the annulus

Figure 9

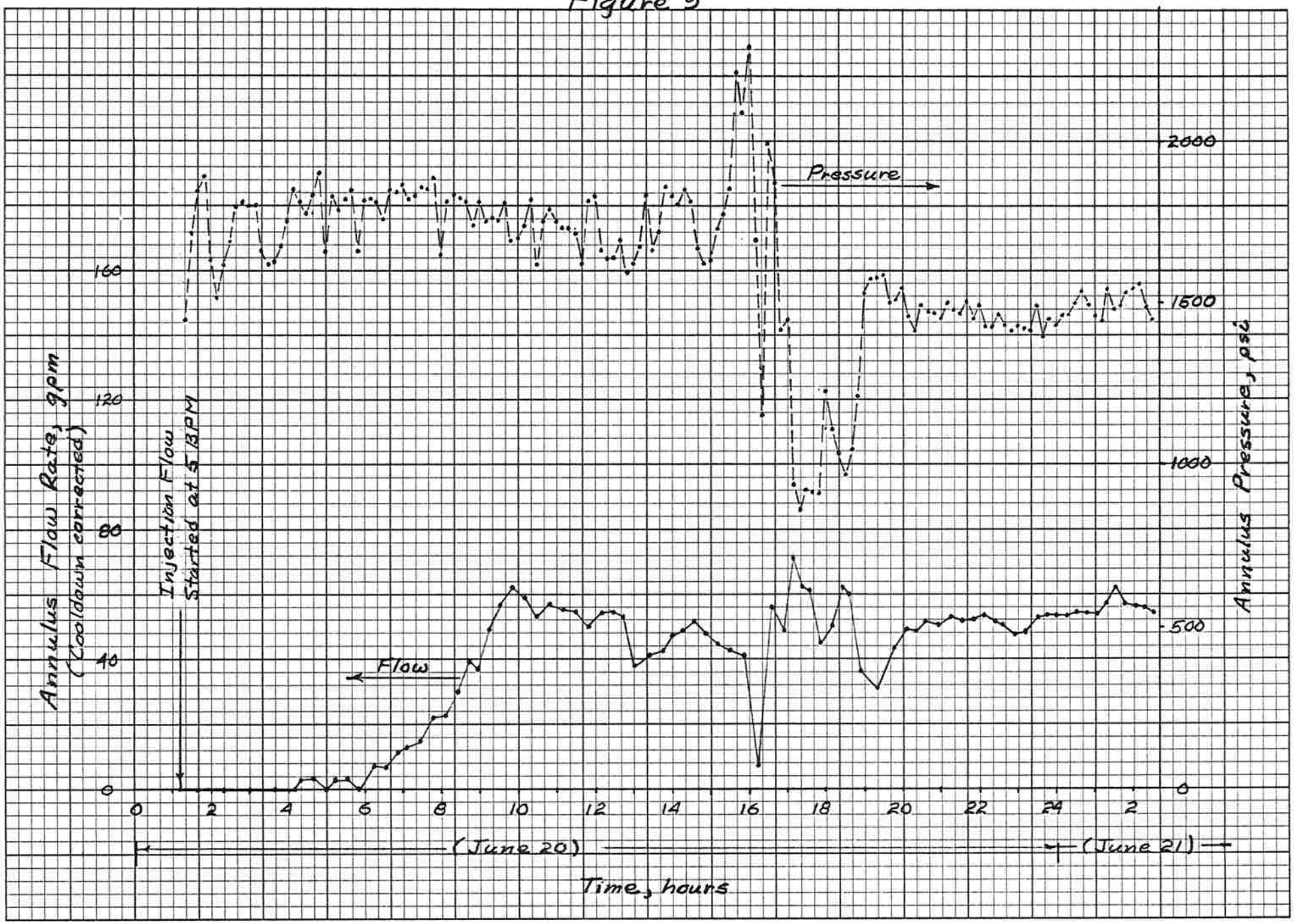

vent flow rate finally stabilized at between 45 and 55 gpm, remaining relatively constant at this level for the remainder of the test, except for a two-hour period discussed later.

Three different sources for this annulus flow have previously been proposed:

1. A leak across the PBR seals
2. Flow up a postulated microannulus between the steel liner and the confining cement
3. Flow through a fracture network connecting the wellbore below the liner to the annulus above the PBR.

A bypass flow leak across the PBR seals now appears very unlikely for several reasons. First, a post-test examination of the pipe string revealed no pipe failures and no apparent flow errosion of the seals (re: John Rowley). Second, at a near-constant (± 200 psi) seal pressure drop of 3700 psi during the first six hours of flow injection during Expt. 2016 (until about 07:40), the behavior of the developing bypass flow is inconsistant with a possible seal leak. A seal leak, if present, would have been expected to develop quickly, with the bypass flow cascading as the seals washed out. Instead, as seen from Fig. 9, the leak appears to have started almost five hours after the driving pressure drop was established, and then to have increased slowly to a near-constant level after nine hours.

A bypass flow path up a cooling-induced microannulus between the steel liner and the cement also seems unlikely. Using conservative input numbers, the cooling-induced microannulus would have had to be at least ten times wider than that proviided by the contraction of the steel alone, to account for the observed 50 gpm bypass flow with a 3700 psi pressure drop.* Further, if the bypass flow were to have been primarily a function of the downhole temperature, it should have developed earlier than it did, and would have reached a maximum value when the bottomhole temperature had

---

* This conclusion is supported by an independent calculation made by George Zyvoloski.

stabilized below about 100°C. However, as shown in Fig. 10, this condition was achieved in only six hours following flow iniitiation, not the nine hours shown in Figure 9.

A flow bypass via a fracture system connecting the openhole section of EE-2 below the liner to the annulus above the PBR appears to be the most probable. The developing bypass flow shown in Fig. 9 exhibits a more-or-less typical diffusional behavior. For the first five hours, while the pressure field was building up out through the fracture network, the outlet flow was negligible. Then, there was a rather rapid increase in bypass flow as the diffusing pressure field reached the fracture intersection with the wellbore in the annulus above the PBR. Finally, as the fluid pressure level in the fracture system in this region stabilized, the bypass flow rate reached a near steady-state value for an approximately constant annulus backpressure level.

This proposed long-time-constant diffusional flow process is supported by other bypass flow behavior. Long after flow shutdown at 01:11 Monday morning, the annulus was still flowing at the same level. At 03:00, the annulus flow rate was about 50 gpm for a reservoir shutin pressure of 5000 psi, and an annulus pressure of about 1500 psi. However, as expected, the bypass flow rate responds rapidly to changes in backpressure (the annulus pressure). Between 16:40 and 18:40, the mean annulus pressure was reduced from 1750 psi to about 1000 psi. At the same time, the bypass flow increased from 48 gpm to 56 gpm. Thus, an 18% increase in the reservoir-to-annulus $_{\Delta}P$ resulted in a 17% flow increase.

If one accepts that the annulus outflow resulted from flow through a fracture system connecting the bottom openhole interval to the annulus above the cemented-in liner (a mean distance of about 700 feet), a fracture flow impedance can be obtained. For an average reservoir-to-annulus pressure drop of 3900 psi and a bypass flow rate of 52 gpm, the specific fracture flow impedance would be 75 psi/gpm. It is interesting to note that this value is very close to the initial Phase I reservoir flow impedance prior to redrilling GT-2.

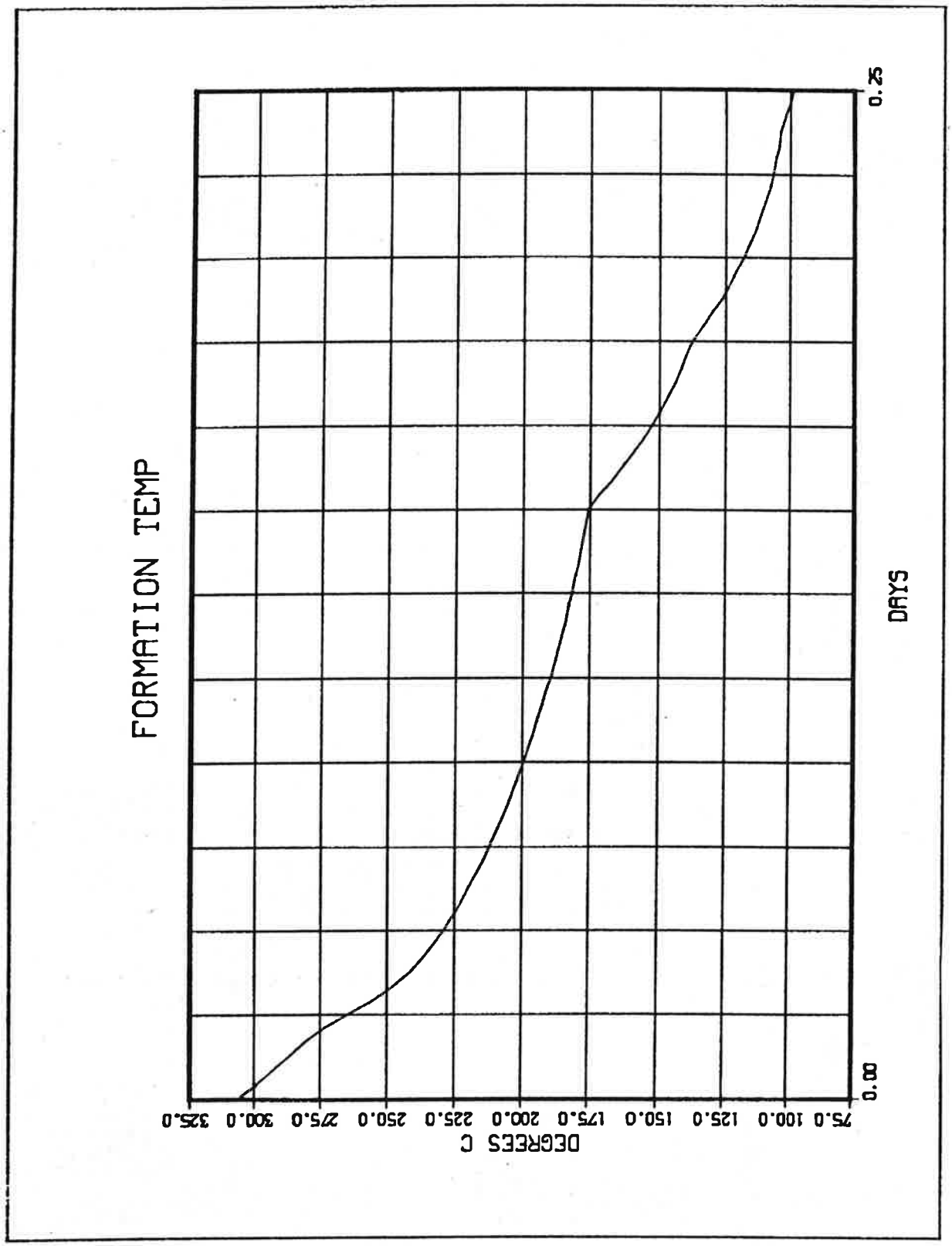

Figure 10. EE-2 Fluid Temperature Profile at a Slant Depth of 14,700 Feet, Obtained From the As-run Injection Flow Profile Shown in Figure 1.

APPENDIX

Mean Fracture Inclination as Inferred from Earth Stress Data (D. Brown)

As discussed previously, the seismic data strongly suggest that we opened a set of inclined fractures near the bottom of EE-2 during Expts. 2012 and 2016. Although the dip of this fracture set is variable as shown in Fig. 4, the mean dip appears to be about 45 degrees.

It is informative to calculate the corresponding fracture dip angle from a completely different approach, using earth stresses. The earth stress situation in the Phase II reservoir -- the openhole sections of EE-2 and EE-3 -- as extrapolated from the Phase I reservoir stress determinations, has previously been presented in memorandum ESS-4-82-4.* From page 6 and the figure on page 2 of this memorandum, the following stress situation is predicted for the bottom of EE-2 at a TVD of 14,100 feet:

σ_3 = 2720 psi

$S_1 = \rho gh$ = 16,180 psi (ρ = 2.65 gm/cc)

P_o = 5560 psi (geothermal gradient)

$\sigma_1 = S_1 - P_o$ = 10,620 psi

Using the measured fracture closure stress (total) of 11,680 psi as given above,

$$\sigma_n = S_n - P_o = 6120 \text{ psi}$$

For θ measured from the horizontal (dip angle):

$$\sigma_n = \sigma_3 \sin^2\theta + \sigma_1 \cos^2\theta$$

$$6120 = 2720 \sin^2\theta + 10{,}620 \cos^2\theta$$

$$\theta = 49°$$

The agreement between these two separate determinations of the fracture inclination is remarkably good.

---

* "The EE-2/EE-3 Compressive Stress Situation," Don Brown, January 14, 1982.